

From Many-Particle Interference to Correlation Spectroscopy

Mattia Walschaers,^{1,2,*} Jack Kuipers,³ and Andreas Buchleitner^{1,†}

¹*Physikalisches Institut, Albert-Ludwigs-Universität Freiburg,
Hermann-Herder-Str. 3, D-79104 Freiburg, Germany*

²*Instituut voor Theoretische Fysica, KU Leuven,
Celestijnenlaan 200D, B-3001 Heverlee, Belgium*

³*D-BSSE, ETH Zürich, Mattenstrasse 26, 4058 Basel, Switzerland*

(Dated: April 10, 2022)

We show how robust statistical features of a many-particle quantum state’s two-point correlations after transmission through a multi-mode random scatterer can be used as a sensitive probe of the injected particles’ mutual indistinguishability. This generalizes Hong-Ou-Mandel interference as a diagnostic tool for many-particle transmission signals across multi-mode random scatterers. Furthermore, we show how, from such statistical features of the many-particle interference pattern, information can be deduced on the temporal structure of the many-particle input state, by inspection of the many-particle interference with an additional probe particle of tuneable distinguishability.

Identical particles are of profound importance in nature: Pauli’s exclusion principle for fermions forms the cornerstone of chemistry, whereas bosonic quantum statistics allows us to prepare Bose-Einstein condensates and induces Planck’s law of black body radiation. As such, quantum statistics describes fundamental symmetry properties of quantum states of identical particles, in equilibrium. Yet, it turns out that the quantum *dynamics* of identical particles holds additional and non-trivial surprises, due to intricate interference phenomena on the level of many-particle transition amplitudes. The simplest manifestation thereof is the by now well-established Hong-Ou-Mandel (HOM) interference dip [1, 2] which is observed when two photons are transmitted through a balanced beam splitter. However, it recently has been realised that HOM is only the tip of the iceberg of a whole zoo of many-particle interference phenomena [3–17], with many particles transmitted through many, randomly coupled modes as the other (truly complex) extreme, of potential relevance for photonic quantum simulation and/or computation [18–22].

Hence, many-particle interference defines a new, wide, and rather unexplored area of quantum effects which may also be considered as novel resources e.g. for quantum information processing [23, 24]. As for all interference phenomena, however, remains the question of their robustness against decoherence effects, with partial distinguishability [9, 10, 20, 25, 26] of the interfering particles as its arguably most prominent source. Again, HOM and many-particle generalisations thereof already provide answers for simple topologies of the coupled modes [4, 8, 12, 13]. But how does partial distinguishability impact on *statistical* quantifiers [27] of many-particle interference, in cases where the complexity of the dynamics (measured by the number of many-particle ampli-

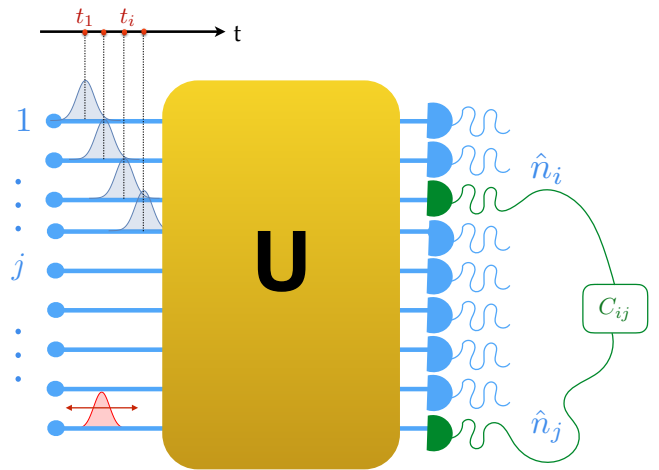


Figure 1. Sketch of the proposed setup. m input modes are connected by a linear optical circuit to m output modes, on each of which a photon counter is mounted. The initial input state to be characterised consists of n (here four – top-most modes on the left) photons which are described by wave packets. The photons are injected at possibly distinct times t_j , what modulates their mutual indistinguishabilities. The two-point truncated correlation function C_{ij} , eq. (4), is the experimental observable to be sampled over all $i \neq j$. A fifth photon (bottom left) may be injected with controlled arrival time, to probe the temporal structure of the four photon input state, through “correlation resonances” e.g. of NM , see eq. (12) and Fig. 3.

tudes which are dynamically superimposed) prevents a deterministic description? And to which extent can also such statistical quantifiers then be employed as diagnostic tools? We here provide the framework for a systematic approach to these questions.

To do so, let us first collect the essential technical tools: Bosonic Fock space is constructed [28, 29] by the vacuum state Ω acted upon by creation operators of type $a_j^\dagger(\psi)$. The latter creates a photon in the j th input mode of the

* mattia@itf.fys.kuleuven.be

† a.buchleitner@physik.uni-freiburg.de

linear optical circuit depicted in Fig. 1, with the argument $\psi \in \mathcal{H}_{\text{add}}$ a state vector from an auxiliary Hilbert space \mathcal{H}_{add} , which summarises all additional degrees of freedom of the photon, such as the temporal structure of the incoming wave packets sketched in the figure. With the adjoint annihilation operators $a_j(\phi)$, the associated commutation relations read [29]

$$[a_i(\phi), a_j^\dagger(\psi)] = \delta_{ij} \langle \phi, \psi \rangle. \quad (1)$$

The action of the optical circuit in Fig. 1 is described by an $m \times m$ unitary matrix U , with m the number of modes:

$$a_j^\dagger(\psi) \mapsto \sum_{k=1}^m U_{jk} a_k^\dagger(\psi), \quad (2)$$

Thus, U mixes the different modes, while leaving the additional degrees of freedom untouched. An initial state of n photons, prepared in n distinct input modes q_1, \dots, q_n , undergoes the dynamical mapping

$$a_{q_1}^\dagger(\psi_1) \dots a_{q_n}^\dagger(\psi_n) \Omega \mapsto \sum_{k_1, k_2, \dots, k_n=1}^m U_{q_1 k_1} \dots U_{q_n k_n} a_{k_1}^\dagger(\psi_1) \dots a_{k_n}^\dagger(\psi_n) \Omega =: \Psi. \quad (3)$$

For n and m sufficiently large, and U lacking any prominent symmetry properties, a deterministic evaluation of Ψ rapidly turns into an intractable problem, and a statistical treatment is needed [16, 27, 30]. We have shown earlier that statistical sampling over the set of two-mode truncated correlation functions

$$C_{ij} := \langle \hat{n}_i \hat{n}_j \rangle_\Psi - \langle \hat{n}_i \rangle_\Psi \langle \hat{n}_j \rangle_\Psi, \quad (4)$$

for all pairs of output modes $i \neq j$, allows to detect robust and characteristic features indicative of the many-particle interferences as induced by U for distinguishable and indistinguishable particles. Here we expand this theory to monitor the continuous (quantum-classical, in the sense of quantum statistics) transition from strictly indistinguishable to fully distinguishable particles, which can be tuned by a continuous degree of freedom accommodated by \mathcal{H}_{add} . Specifically, we choose this degree of freedom as given by the photon arrival times t_j , $j = 1, \dots, n$ (see Fig. 1).

To evaluate (4) while taking account of the temporal degree of freedom attached to each of the interfering photons, we define the single mode number operators on output by

$$\hat{n}_i := \sum_k a_i^\dagger(\eta_k) a_i(\eta_k), \quad (5)$$

where the η_k form a basis of \mathcal{H}_{add} [31]. The explicit

expression for (4) then reads

$$C_{ij} = \sum_{k \neq l=1}^n |\langle \psi_k, \psi_l \rangle|^2 U_{q_k i} U_{q_l j} U_{q_i}^* U_{q_k j}^* - \sum_{k=1}^n U_{q_k i} U_{q_k j} U_{q_k i}^* U_{q_k j}^*, \quad (6)$$

with ψ_k the k th photon's wave function in the temporal degree of freedom. The overlap $|\langle \psi_k, \psi_l \rangle|^2$, tantamount of the degree of indistinguishability of the k th and l th photon (with values between one and zero), gives a tuneable weight to the two-particle interference term in (6), and thus continuously interpolates between the fully indistinguishable ($|\langle \psi_k, \psi_l \rangle|^2 = 1$) and the fully distinguishable ($|\langle \psi_k, \psi_l \rangle|^2 = 0$, for all $k \neq l$) case.

Given that the statistics, and, in particular, the lowest order moments of the *C-dataset* [27] (defined as the sample of all C_{ij} , $i \neq j$) define unambiguous benchmarks for many-particle interference of (in-)distinguishable particles, (6) now is the fundamental building block to derive analytic expressions for those lowest order moments for arbitrary choices of the injected photons' mutual indistinguishabilities $|\langle \psi_k, \psi_l \rangle|^2$. The normalised mean (*NM*) and the coefficient of variation (*CV*) of the C-dataset given by

$$NM := \frac{m^2}{n} M_1, \quad (7)$$

$$CV := \frac{\sqrt{M_2 - M_1^2}}{M_1}, \quad (8)$$

with

$$M_1 := \frac{2}{m(m-1)} \sum_{i < j=1}^m C_{ij}, \quad (9)$$

$$M_2 := \frac{2}{m(m-1)} \sum_{i < j=1}^m (C_{ij})^2, \quad (10)$$

together with the overlap of Gaussian photonic wave packets, centred at t_j with spectral width $\Delta\omega$,

$$|\langle \psi_k, \psi_l \rangle|^2 = \exp\left(-\frac{\Delta\omega^2 (t_k - t_l)^2}{2}\right), \quad (11)$$

lead to the following explicit random matrix theory [32] (RMT) predictions, for U given by a random unitary matrix chosen from the Haar measure [33–37]:

$$NM \approx \mathbb{E}_U(C_{ij}) \frac{m^2}{n} = -\frac{m}{m+1} \left(1 + \frac{1}{n(m-1)} \sum_{k \neq l=1}^n \exp\left(-\frac{\Delta\omega^2 (t_k - t_l)^2}{2}\right) \right), \quad (12)$$

and

$$\begin{aligned} \overline{NM} &\approx \mathbb{E}_U \left(\overline{C_{ij}} \right) \frac{m^2}{n} \\ &= -\frac{m}{m+1} \left(1 + \frac{n-1}{\sqrt{1+2(\Delta\omega\delta t)^2(m-1)}} \right). \end{aligned} \quad (13)$$

NM predicts the normalized mean for well-defined injection times t_k , while \overline{NM} assumes independently (normal) distributed photonic arrival times t_k with zero mean and width δt , hence implies an additional statistical average over the arrival times. The corresponding, more involved expressions for CV and \overline{CV} are given in the Supplementary Material.

Let us first compare the RMT prediction (13) for \overline{NM} to numerically generated results which are obtained by direct evaluation of (9) and (10), *i.e.* as the averages over all possible choices of output modes of a fixed random circuit U , and over Gaussian distributed t_k , $k = 1, \dots, n$, with variable δt and fixed $\Delta\omega$. Fig. 2 shows the *statistical* analog of the HOM dip, as exhibited by both, \overline{NM} and \overline{CV} . RMT prediction and numerical simulation agree very well. Note that residual fluctuations of the numerical result around the RMT prediction, more prominent for the coefficient of variation, will be progressively suppressed in the thermodynamic limit. The visibility of the dip is given by the difference between the results for the distinguishable and indistinguishable case, with known scaling behaviour in n and m [27]. Hence, much as in the HOM setting, but now for *large* n and m and for *unknown, random* U does this result define a diagnostic tool for the experimental certification of the indistinguishable preparation of the injected photons.

Next, we exploit the structure of (12) to establish how the C-dataset can be used to probe the temporal structure of the *many*-particle input state by manipulating a *single* photon's input state: Assume that the injection times of the first $n-1$ photons be fixed, and that the n th photon's injection time be controllable by an adjustable delay line. Then, by virtue of the sum of exponentials in (12) (and, likewise, in the corresponding expressions (16 - 20, 26) in the Supplementary Materials for CV), whenever $t_n \simeq t_k$, $n \neq k$, the thus triggered two-photon interference between photons n and k will induce a dip in NM , of width $\Delta\omega^{-1}$, centred around t_k , much as in a typical spectroscopic experiment. This protocol thus even allows to infer (with finite resolution controlled by the photons' spectral bandwidth) the actual timing of the injected photons. Again, as shown in Fig. 3, RMT results and numerical simulations agree qualitatively very well, with some quantitative deviations in the vicinity of the minima of NM . We attribute these to the difference between the RMT average (12) and the contribution of the "correlation resonance" between the probe and the k th input photon to the signal as generated by a specific realisation of U .

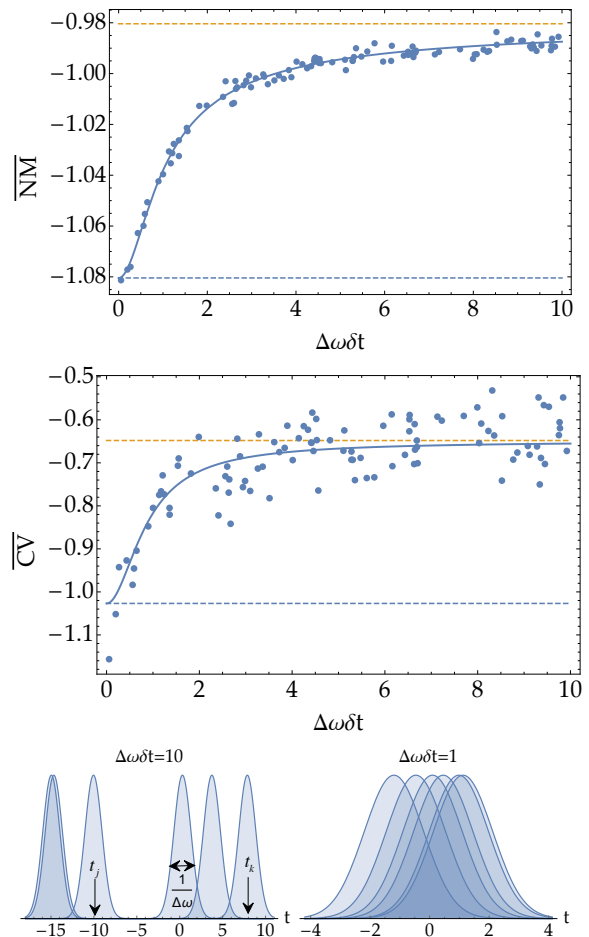


Figure 2. Normalised mean (NM , top, eq. (7)) and coefficient of variation (CV , middle, eq. (8)) of the C-dataset generated by the transmission of $n = 6$ photons across a $m = 50$ mode random unitary, as a function of the temporal scatter δt of the photons' (normally distributed, with zero mean) arrival times t_j , at given spectral width $\Delta\omega$. The bottom plot sketches two typical scenarios. Continuous lines indicate the RMT predictions (13) and (21 - 26), while dots are derived from a numerically generated C-dataset, with one single, fixed random realisation of U , and upon average over 100 normally distributed arrival times per t_j . The difference between the predictions for strictly indistinguishable bosons and for distinguishable particles (horizontal dotted lines) determine the visibility of the signal.

We finally stress that the statistical characterisation of the quantum-classical transition as here proposed can also be applied to structured or highly symmetric circuits such as described by Fourier matrices. This type of circuits exhibit prominent interference effects which have been experimentally demonstrated very recently [38] and can be understood analytically [6, 11, 39]. Consequently, also the C_{ij} and, subsequently, NM can be directly evaluated, *without* recourse to RMT. NM is a remarkably robust quantity for the Fourier circuit, since it is independent of the specific input modes which are chosen.

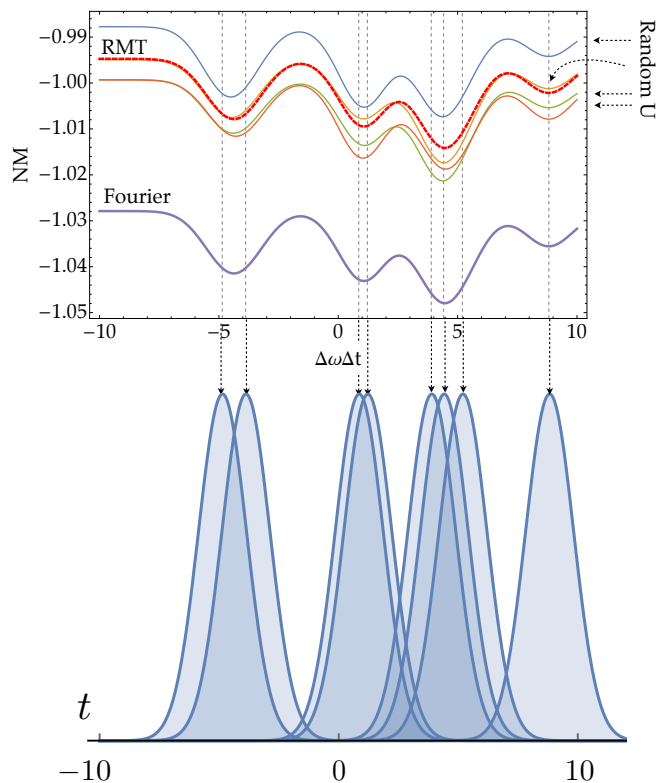


Figure 3. Normalised mean NM , as a function of the probe photon's (see Fig. 1) delay with respect to $t = 0$, and for $n - 1 = 8$ injected photons with injection times $t_k = -4.86071, -3.87957, 0.858186, 1.21835, 3.89386, 4.41308, 5.19717, 8.82249$ (in units of $1/\Delta\omega$), for numerically generated, random (thin lines) $m = 30$ mode unitaries, compared to the RMT prediction (12) (thick, dashed red line), and to the result (31) for the Fourier circuit. Clearly, whenever the probe photon's delay coincides with any one of the other photons' injection times (associated wave packets are displayed in the bottom panel), a resonance-like dip emerges in the C-dataset's lowest order statistical moment.

We find, with (7,9)

$$NM = -1 - \frac{1}{n(m-1)} \sum_{k \neq l=1}^n \exp\left(\frac{\Delta\omega^2(t_k - t_l)^2}{2}\right), \quad (14)$$

with a slightly increased visibility of the signal displayed in Fig. 3, as compared to the result for a random scatterer.

Let us conclude with the observation that the treatment of many-particle interference phenomena in terms of a set of correlators with statistical properties which are indicative of structural properties of the injected quantum states defines a new type of *correlation spectroscopy*. While we did here focus on the photonic context which originally motivated this work, the underlying theoretical structure as incarnated by (6) is rather general and lends itself to straightforward gener-

alisations to other “distinguishing” degrees of freedom, as well as to other, e.g. fermionic particle species. Since the overlaps $|\langle\psi_k, \psi_l\rangle|^2$ in the distinguishing degree of freedom define some sort of which-way information on the level of two-particle transition amplitudes, this furthermore indicates new directions for the decoherence theory of quantum systems of indistinguishable particles.

Acknowledgements The authors thank Juan Diego Urbina and Klaus Richter for fruitful discussions. M.W. expresses gratitude to the German National Academic Foundation for financial support. A.B. acknowledges support by the EU Collaborative project QuProCS (Grant Agreement 641277).

-
- [1] C. K. Hong, Z. Y. Ou, and L. Mandel, Phys. Rev. Lett. **59**, 2044 (1987).
 - [2] Y. H. Shih and C. O. Alley, Phys. Rev. Lett. **61**, 2921 (1988).
 - [3] R. A. Campos, B. E. A. Saleh, and M. C. Teich, Phys. Rev. A **40**, 1371 (1989).
 - [4] A. V. Belinskii, D. N. Klyshko, and M. E. Alferieff, Soviet physics, JETP **75**, 606 (1992).
 - [5] Y. L. Lim and A. Beige, New J. Phys. **7**, 155 (2005).
 - [6] M. C. Tichy, M. Tiersch, F. de Melo, F. Mintert, and A. Buchleitner, Phys. Rev. Lett. **104**, 220405 (2010).
 - [7] K. Mayer, M. C. Tichy, F. Mintert, T. Konrad, and A. Buchleitner, Phys. Rev. A **83**, 062307 (2011).
 - [8] M. C. Tichy, H.-T. Lim, Y.-S. Ra, F. Mintert, Y.-H. Kim, and A. Buchleitner, Phys. Rev. A **83**, 062111 (2011).
 - [9] M. C. Tichy, *Entanglement and interference of identical particles*, PhD Thesis, Albert-Ludwigs Universität Freiburg, Freiburg (2011).
 - [10] K. Mayer, *Many-particle Quantum Walks*, Diploma Thesis, Albert-Ludwigs Universität Freiburg, Freiburg (2012).
 - [11] M. C. Tichy, M. Tiersch, F. Mintert, and A. Buchleitner, New J. Phys. **14**, 093015 (2012).
 - [12] Y.-S. Ra, M. C. Tichy, H.-T. Lim, O. Kwon, F. Mintert, A. Buchleitner, and Y.-H. Kim, PNAS **110**, 1227 (2013).
 - [13] Y.-S. Ra, M. C. Tichy, H.-T. Lim, O. Kwon, F. Mintert, A. Buchleitner, and Y.-H. Kim, Nat Commun **4** (2013), 10.1038/ncomms3451.
 - [14] S. Laibacher and V. Tamma, Phys. Rev. Lett. **115**, 243605 (2015).
 - [15] V. Tamma and S. Laibacher, Phys. Rev. Lett. **114**, 243601 (2015).
 - [16] M. Walschaers, F. Schlawin, T. Wellens, and A. Buchleitner, Annual Review of Condensed Matter Physics **7**, 223 (2016).
 - [17] J.-D. Urbina, J. Kuipers, S. Matsumoto, Q. Hummel, and K. Richter, Phys. Rev. Lett. **116**, 100401 (2016).
 - [18] M. Bentivegna, N. Spagnolo, C. Vitelli, F. Flamini, N. Viggianiello, L. Latmiral, P. Mataloni, D. J. Brod, E. F. Galvao, A. Crespi, R. Ramponi, R. Osellame, and F. Sciarrino, Sci. Adv. **1**, e1400255 (2015).
 - [19] M. A. Broome, A. Fedrizzi, S. Rahimi-Keshari, J. Dove, S. Aaronson, T. C. Ralph, and A. G. White, Science

- 339**, 794 (2013).
- [20] N. Spagnolo, C. Vitelli, M. Bentivegna, D. J. Brod, A. Crespi, F. Flamini, S. Giacomini, G. Milani, R. Ramponi, P. Mataloni, R. Osellame, E. F. Galvão, and F. Sciarrino, *Nat Photon* **8**, 615 (2014).
- [21] J. B. Spring, B. J. Metcalf, P. C. Humphreys, W. S. Kolthammer, X.-M. Jin, M. Barbieri, A. Datta, N. Thomas-Peter, N. K. Langford, D. Kundys, J. C. Gates, B. J. Smith, P. G. R. Smith, and I. A. Walmsley, *Science* **339**, 798 (2013).
- [22] M. Tillmann, B. Dakić, R. Heilmann, S. Nolte, A. Szameit, and P. Walther, *Nat Photon* **7**, 540 (2013).
- [23] M. J. Bremner, R. Jozsa, and D. J. Shepherd, *Proc. R. Soc. A*, rspa20100301 (2010).
- [24] S. Aaronson and A. Arkhipov, *Theory of Computing* **9**, 143 (2013).
- [25] V. S. Shchesnovich, *Phys. Rev. A* **91**, 013844 (2015).
- [26] M. C. Tichy, *Phys. Rev. A* **91**, 022316 (2015).
- [27] M. Walschaers, J. Kuipers, J.-D. Urbina, K. Mayer, M. C. Tichy, Klaus Richter, and A. Buchleitner, *New J. Phys.* **18**, 032001 (2016).
- [28] O. Bratteli and D. W. Robinson, *Operator algebras and quantum statistical mechanics equilibrium states. Models in quantum statistical mechanics* (Springer, Berlin, 1997).
- [29] R. Alicki, in *Quantum Information, Computation and Cryptography*, Lecture Notes in Physics No. 808, edited by F. Benatti, M. Fannes, R. Floreanini, and D. Petritis (Springer Berlin Heidelberg, 2010) pp. 151–174.
- [30] M. Walschaers, *Efficient Quantum Transport*, PhD Thesis (submitted), Albert-Ludwigs-Universität Freiburg & KU Leuven, Freiburg (2016).
- [31] Note that this definition of the number operators implies that the detectors in Fig. 1 do integrate over the photon arrival times.
- [32] M. L. Mehta, *Random Matrices* (Elsevier/Academic press, Amsterdam, 2004).
- [33] S. Samuel, *Journal of Mathematical Physics* **21**, 2695 (1980).
- [34] P. A. Mello, *J. Phys. A: Math. Gen.* **23**, 4061 (1990).
- [35] P. W. Brouwer and C. W. J. Beenakker, *J. Math. Phys.* **37**, 4904 (1996).
- [36] B. Collins and P. Śniady, *Commun. Math. Phys.* **264**, 773 (2006).
- [37] G. Berkolaiko and J. Kuipers, *Journal of Mathematical Physics* **54**, 112103 (2013).
- [38] A. Crespi, R. Osellame, R. Ramponi, M. Bentivegna, F. Flamini, N. Spagnolo, N. Viggianiello, L. Innocenti, P. Mataloni, and F. Sciarrino, *Nat Commun* **7**, 10469 (2016).
- [39] M. C. Tichy, K. Mayer, A. Buchleitner, and K. Mølmer, *Phys. Rev. Lett.* **113**, 020502 (2014).

Supplementary Materials

RMT Predictions

In this section we present additional information on the RMT averaging over the Haar measure on the unitary group. The key identity used to perform these averages reads [33–37]

$$\mathbb{E}_U(U_{a_1, b_1} \cdots U_{a_n, b_n} U_{\alpha_1, \beta_1}^* \cdots U_{\alpha_n, \beta_n}^*) = \sum_{\sigma, \pi \in S_n} V_m(\sigma^{-1}\pi) \prod_{k=1}^n \delta(a_k - \alpha_{\sigma(k)}) \delta(b_k - \beta_{\pi(k)}), \quad (15)$$

for the average over $m \times m$ unitary matrices. The functions $V_m(\sigma^{-1}\pi)$ in (15) can be obtained via different methods, as shown in [35, 36]. We combine (15) with the expression (6) for C_{ij} to straightforwardly evaluate NM (12) and \overline{NM} (13).

In addition, (15) allows us to evaluate CV and \overline{CV} . We use the results from [35] in a long but straightforward computation, and obtain

$$\begin{aligned} \mathbb{E}_U(C_{ij}^2) &= \frac{2A - 2B(m-5) + 2D(2+6m-n+mn) + C(10+m+m^2)}{(m-1)m^2(m+1)(m+2)(m+3)} \\ &+ \frac{(m-2)(1+3m)n + 2n^2 + mn^2 + m^2n^2}{(m-1)m^2(m+1)(m+2)(m+3)}, \end{aligned} \quad (16)$$

with

$$A = \sum_{\substack{k_1, k_2, l_1, l_2=1 \\ k_1 \neq k_2 \neq l_1 \neq l_2}}^n |\langle \psi_{k_1}, \psi_{l_1} \rangle|^2 |\langle \psi_{k_2}, \psi_{l_2} \rangle|^2, \quad (17)$$

$$B = \sum_{\substack{k, l_1, l_2=1 \\ k \neq l_1 \neq l_2}}^n |\langle \psi_k, \psi_{l_1} \rangle|^2 |\langle \psi_k, \psi_{l_2} \rangle|^2, \quad (18)$$

$$C = \sum_{\substack{k, l=1 \\ k \neq l}}^n |\langle \psi_k, \psi_l \rangle|^4, \quad (19)$$

$$D = \sum_{\substack{k, l=1 \\ k \neq l}}^n |\langle \psi_k, \psi_l \rangle|^2. \quad (20)$$

Moreover, we find that

$$\begin{aligned} \mathbb{E}_U(\overline{C_{ij}^2}) &= \frac{2A' - 2B'(m-5) + 2D'(2+6m-n+mn) + C'(10+m+m^2)}{(m-1)m^2(m+1)(m+2)(m+3)} \\ &+ \frac{(m-2)(1+3m)n + 2n^2 + mn^2 + m^2n^2}{(m-1)m^2(m+1)(m+2)(m+3)}, \end{aligned} \quad (21)$$

with

$$A' = \frac{n(n-1)(n-2)(n-3)}{(1+2(\Delta\omega\delta t)^2)}, \quad (22)$$

$$B' = \frac{n(n-1)(n-2)}{(1+2(\Delta\omega\delta t)^2)}, \quad (23)$$

$$C' = \frac{n(n-1)}{(1+2(\Delta\omega\delta t)^2)}, \quad (24)$$

$$D' = \frac{n(n-1)}{\sqrt{1+2(\Delta\omega\delta t)^2}}. \quad (25)$$

We can combine these outcomes with the results for NM (12) and \overline{NM} (13) to determine

$$CV = \frac{\sqrt{\mathbb{E}_U(C_{ij}^2) - \mathbb{E}_U(C_{ij})^2}}{\mathbb{E}_U(C_{ij})}, \quad \text{and} \quad \overline{CV} = \frac{\sqrt{\mathbb{E}_U(\overline{C_{ij}^2}) - \mathbb{E}_U(\overline{C_{ij}})^2}}{\mathbb{E}_U(\overline{C_{ij}})}. \quad (26)$$

The latter leads to the RMT prediction for the second panel in Fig. 2.

Correlators for the Fourier Matrix

Expression (31) for the normalised mean of the Fourier circuit C-dataset is obtained via a direct evaluation of (9), with U a Fourier matrix, hence

$$U_{q_k i} = \frac{1}{\sqrt{m}} \exp\left(2\pi i \frac{(q_k - 1)(i - 1)}{m}\right). \quad (27)$$

We may now write (6) as

$$C_{ij} = -\frac{n}{m^2} - \frac{1}{m^2} \sum_{k \neq l=1}^n |\langle \psi_k, \psi_l \rangle|^2 \exp\left(2\pi i \frac{(q_l - q_k)(j - i)}{m}\right), \quad (28)$$

which needs to be averaged over all output modes i and j to obtain M_1 (9). When we consider a fixed value i , we obtain that

$$\sum_{\substack{j=1 \\ j \neq i}}^m \exp\left(2\pi i \frac{(q_l - q_k)j}{m}\right) = -\exp\left(2\pi i \frac{(q_l - q_k)i}{m}\right). \quad (29)$$

The identity (29) implies

$$\sum_{\substack{i,j=1 \\ i \neq j}}^m \exp\left(2\pi i \frac{(q_l - q_k)(j - i)}{m}\right) = -m, \quad (30)$$

and hence, with (7, 9), one obtains

$$NM = -1 - \frac{1}{n(m-1)} \sum_{k \neq l=1}^n |\langle \psi_k, \psi_l \rangle|^2. \quad (31)$$